Post-Earthquake Fire Simulation of Steel Structures: Modelling features using *OpenSees*

Rita de Almeida Palma

Instituto Superior Técnico, Universidade de Lisboa

Janeiro 2021

ABSTRACT

Events such as earthquakes and fires can cause severe consequences, in terms of life and property losses. Cascading events like post-earthquake fires (PEF) increase the damage caused by the earthquake alone, mainly due to the fact that damaged structures are more vulnerable to the fire effects, than the undamaged ones. Thus, PEF is often responsible for additional damage to buildings.

The current work is focused on investigating the influence of the damage induced by a seismic event on the fire resistance of a steel structure. A benchmark case is considered, and by performing several analyses assuming different fire scenarios, earthquakes and nonlinear frame element models, recommendation on the development of such analysis are provided.

Results of different frame element models, which are developed in the *OpenSees (Open System for Earthquake Engineering Simulation)* platform, are compared in order to demonstrate the influence of different modeling choices in what concerns seismic behavior assessment.

Existing models and analysis of steel frame structures in fire are explored, which are suitable to the case study example used herein. Criteria to evaluate structural resistance, based on EN1998-3, is proposed and tested in the scope of the case study.

Finally, the PEF scenario is analyzed considering a couple of seismic events and two fire scenarios. Comparison is made between the response of damaged and undamaged structure.

Keywords:

Earthquake, Fire, Post-Earthquake fire, Seismic Analysis, Fire Analysis, Nonlinear Static Analysis, Nonlinear Dynamic Analysis, Thermomechanical Analysis, OpenSees, Steel Structures

1 Introduction

Passive fire protection design measures have been criticized due to the serious consequences resulting from large scale fires. Therefore, current codes have started to include design principles on this phenomenon, based on deterministic and probabilistic methods.

However, current design procedures do not account for the concomitant or cascading occurrence of accidental actions, events such as flood following a hurricane, or post-earthquake fire (PEF), which has so far been justified by the low probability of occurrence, as well as the complexity that such analysis would require. Nevertheless, the consequences of these events, in terms of life safety and property loss, may be high [4].

In PEF situations, even when no fire develops immediately after an earthquake, the possibility of later fires affecting the structure must be adequately taken into account, since the earthquake induced damage make the structure more vulnerable to fire effects [13]. The causes that may trigger a fire during or just after an earthquake are numerous, for example electrical and gas related failures, overturning or displacement of heat structures, are among the most common fire triggering events. [12]

The threat posed by PEF has been highlighted by earthquakes like that hit San Francisco, USA, in 1906, and that struck Kanto, Japan, in 1923, respectively, were magnitude 7.9 Mw and

8.2 Mw. In these cases, PEFs were responsible for approximately 80% of the total damage. In the first, amounting to a burnt area of 12.2 km^2 and 28 000 buildings, whereas the second event resulted in 140 000 fatalities and a burnt area of 38.3 km^2 [1].

Since the current seismic design philosophy allows for plastic damage of the load-bearing structure, while the fire design is carried out by assuming undamaged structural elements, a reduced fire resistance of a building subjected to a prior earthquake may be expected. Therefore, the development of design methodologies and procedures that account for these phenomena is deemed necessary [4]. Although in recent studies this problem has been investigated, there are no established methods to evaluate the earthquake impact in the response of steel structures subjected to fire.

Most of the research on PEFs has been performed during the past decades. The vast majority of published numerical studies indicate that PEFs significantly influence the structural integrity of steel buildings, such as *Della Corte et al.* [3]. and *Benham* and *Ronagh* [2], demonstrated that the sequential analysis is the functional tool to consider the effects of residual deformations from an earthquake as well as degradation in stiffness and strength.

The resistance of the structure under fire action is commonly quantified by the time of collapse. This is the case when nominal fire models, such as ISO curves [20], are used. In this model, the time of collapse represents a pseudo time, directly related to the maximum allowable temperature for a structural member. In case of a PEF.

In the last decades, numerical tools have been developed to simulate the non-linear structural response under fire scenarios. In 1997, an open source software framework, Open System for Earthquake Engineering Systems *(OpenSees)* was developed at the University of California, Berkeley, by McKenna [8]. It was initially designed to simulate non-linear response of structural frames under seismic excitations. In 2009, *OpenSees* was adopted at the University of Edinburgh to further develop it to perform structural fire analysis. Significant contributions in terms of heat transfer and fire modules have been made to the framework in developing the 'Thermal' version of *OpenSees* [5].

2 Seismic analysis of steel structures using *OpenSees*

One of the main issues in the PEF analysis is the assessment of the mechanical and geometric residual state of the structure at the end of the earthquake, which represents the initial state for fire action. For the development of a structural model, there is the need to consider: *(i)* the material behavior model and *(ii)* the finite element model.

This chapter presents the modeling process of an example structure in *OpenSees.* Where the main focus is in the differences between the global and local results of three types of finite element models used: *(i)* concentrated plasticity hinge model (CPH), *(ii)* distributed plasticity with force formulation elements model (DFFM), and *(iii)* distributed plasticity with displacement formulation elements model (DDFM), executing static (pushover) and dynamic nonlinear analyses.

2.1 Seismic Methods

Seismic damage is mainly related to: *(i)* "geometrical" damage and *(ii)* "mechanical" damage. The former, which corresponds to the change of the initial structure geometry owing to the residual deformation produced by plastic excursions during the cyclic earthquake response. Otherwise, the latter is the degradation of mechanical properties of those structural components engaged in the plastic range of deformation during the earthquake response [3].

Nonlinear seismic analysis methods consider the plastic behavior of structures, described by nonlinear force-displacement relationships and allowing large deformations if the structure presents high levels of ductility. Pushover analysis is characterized by the computation of a capacity curve, which describes the response of the structure for different levels of deformation, and is usually represented as the normalized base shear (base shear divided by the structure's weight) as a function of the displacement in the control node. In this method, using a specific load pattern, the structure is pushed to arrive at a defined target displacement. The target displacement is determined from the design elastic response spectrum, of an equivalent system of a degree of freedom, 1 DOF.

On the other hand, nonlinear dynamic analysis runs through several seismic accelerograms, either recorded during real earthquakes or

artificially (numerically) derived. Although the depth of information on the structural performance makes this method the reference method for seismic analysis, its complexity and computational cost makes alternative methods, such as the pushover analysis, more and more used.

However, the applicability of pushover analysis for PEF is limited. In fact, in the pushover analysis the residual state of the structure corresponds to that associated with the target displacement. This is a disadvantage of the method, considering that the goal is to obtain a realistic residual state of the structure at the end of the seismic action. Nevertheless, with the capacity curve it can be assessed any resistance capability as function of the drift in the control node or considering cyclic pushover analysis. However, the dynamic response of the structure is lost.

After all, the nonlinear dynamic analysis, allows to introduce fire at any instant of the earthquake action. And since this analysis goes through a history of accelerations, any state corresponds to a realistic situation of a structure response. Consequently, it seems more adequate to PEF events simulation.

2.2 Finite Element and Material Models using *OpenSees*

Material models are typically based on either "mechanical" or "phenomenological" laws. Mechanical models account for the actual non-linear mechanisms, the fiber-section model is the best known and most widely used section mechanical model. It discretizes the beam or column cross section into fibers. Otherwise, in the phenomenological model, the section non-linearities are described by non-linear moment-curvature or moment-rotation laws. This model has the advantage of being calibrated from experimental data, to account for cyclic degradation and local buckling of elements, which are aspects that the mechanical models do account for [10].

In this study, it was used common approaches of steel structural modelling. *Lignos and Krawinkler* [7] phenomenological model was combined with the finite element CPH model, while *Giuffré-Menegotto-Pinto* mechanical model was implemented with the finite element distributed plasticity models, DFFM e DDFM. These are summarized in Table 1, with the *OpenSees* commands, respectively.

In the first material model, beams and columns are made of two zero-length hinges located at the frame elements' two ends and connected by elastic frame elements. Since the elastic element and the two hinges are in series, the beam and column stiffnesses are adjusted using the stiffness ratio $n = k_s/k_e$, where k_s and k_e are the spring stiffness and the elastic element stiffness, respectively [10]. This model, applied to the hinges, address asymmetric component hysteretic behaviour, including different rates of cyclic deterioration in the two loading directions [7], as shown in Figure 1.

In the second material model, is a bilinear model with isotropic strain hardening, including the *Bauschinger* effect, that provides an accurate representation of the steel hysteretic response, as shown in Figure 2.

Table 1 – Summary of Finite Element and Material Models.

Finite Element Model		**Material Model**	
Model	*OpenSees* commands	Model	*OpenSees* commands
CPH	Rigid-plastic hinges*: zeroLength elements*	Phenomenological model: *Modified Ibarra Krawinkler Deterioration Model*	*Bilin uniaxialMaterial*
	Interior elements: *elasticBeamColumn elements*	Linear Elastic	*Elastic uniaxialMaterial*
DFFM	*forceBeamColumn elements*	Mechanical model: *Giuffré-Menegotto-Pinto*	*Steel02 uniaxialMaterial*
DDFM	*dispBeamColumn elements*		

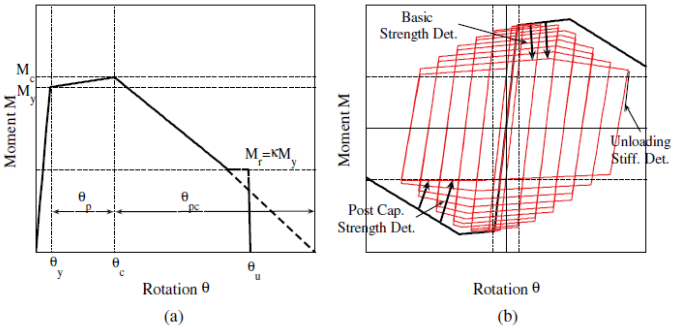

Figure 1 – Lignos and Krawinkler deterioration model: (a) monotonic curve; (b) cyclic curve.

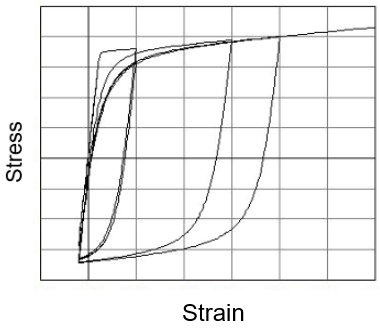

Figure 2 – Stress-strain relationship of the mechanical model.

2.2.1 Description of the structure

The 2-story, 1-bay steel moment resisting frame, is linked to a leaning column with gravity loads by truss elements to simulate P-delta effects. The basic geometry of the frame is presented in Figure 3 and Figure 4, as well as, the modelling representation of each finite element model, respectively, CPH and distributed plasticity models. The distributes design vertical loads are at the second floor: 260.26 kN/m; and at the third floor: p_{sd} =255.39 kN/m. The beams and columns cross-section are W27x102 and W24x131, respectively.

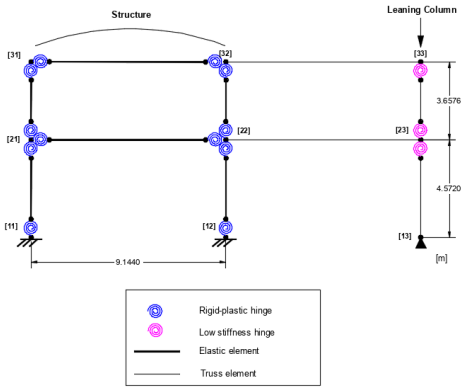

Figure 3 – CPH modelling structure.

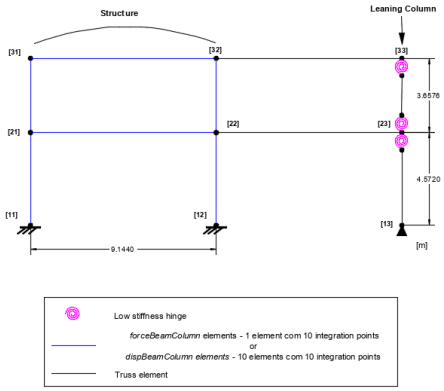

Figure 4 – DFFM and DDFM modelling structure

2.3 Collapse criteria

The global criteria, for the pushover analysis, corresponds to the capacity curve's ultimate drift, defined as the point where 80% of base shear force maximum value is attained, according to NP EN 1998-3 [17]. For the dynamic analysis it was considered, as the global criteria, the drift at the control node that corresponds to the value ultimate drift value defined at the capacity curve, in the pushover analysis.

The local criteria is defined considering the plastic rotation capacity of the columns, according with the actualization of NP EN 1998-3, proposed by *Lignos and Hartloper* [6]. This rotation capacity is presented in the Equation (1) and Equation (2), respectively, for monotonic and cyclic analysis.

$$\theta^{p}_{u,mon} = 296.75 \cdot \left(\frac{h_1}{t_w}\right)^{-1.4} \cdot \left(\frac{L_b}{i_z}\right)^{-0.8} \cdot (1 - v_G)^{2.7} \leq 0.15 \text{ rad} \quad (1)$$

$$\theta^{p}_{u,cic} = 7{,}37 \cdot \left(\frac{h_1}{t_w}\right)^{-0.95} \cdot \left(\frac{L_b}{i_z}\right)^{-0.5} \cdot (1 - v_G)^{2.4} \leq 0.15 \text{ rad} \quad (2)$$

where: h_1, web height with constant thickness of the cross-section; t_w, web thickness of the cross section; L_b, unbraced length of column; i_z, radius of gyration about the weak axis of the steel cross-section; v_G, axial load ratio.

2.4 Results

2.4.1 Pushover Analysis

The capacity curve of the pushover analysis, until the global and local collapse criterion are reached, is shown in Figure 5. As expected, the ultimate drift is almost the same at both distributed plasticity models, because it was imposed the same criteria and the post-capping slope as the same isotropic hardening. Whereas the CPH model due to the degradation parameters, calibrated from experimental data, accentuated the post-capping slope, result in conditioning global collapse criteria, comparing with the distributed plasticity models. However, the local collapse limitation is quite similar between every models. It is also important to say that the critical elements for the local collapse criteria were the columns of the first floor in every model.

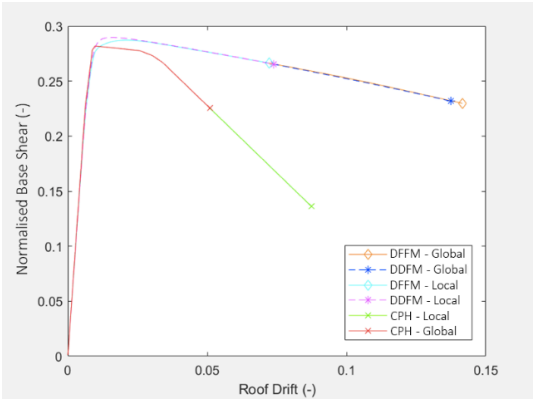

Figure 5 – Capacity curve.

For local level analysis it is presented the moment-curvature curves: at the left end of the first-floor beam, and the bottom end of the column at the first floor, as shown at Figure 6. The differences in the results between the models were caused by the same reason described in the capacity curve. It is observed that the distributed plasticity models reach higher curvatures when the global criteria are achieved. For the local criteria, it is achieved in both models for the same curvature. However, in the beam curve, the distributed plasticity models present higher curvatures than the concentrated plasticity model, more specifically the distributed plasticity model with force formulation. It is verified that the local criteria are reached in the critical section of the column before being reached at the beam.

In an additional sensitivity analysis it was shown that for the same drift roof (4%) at the capacity curve, at the local moment-curvature curves it can be observed that the local response is very different (at the beam and at the column) with the DFFM presenting the highest curvatures, and the CPH model the lowest, being circa 35% and 64% of the curvature of DFFM, respectively, beam and column results.

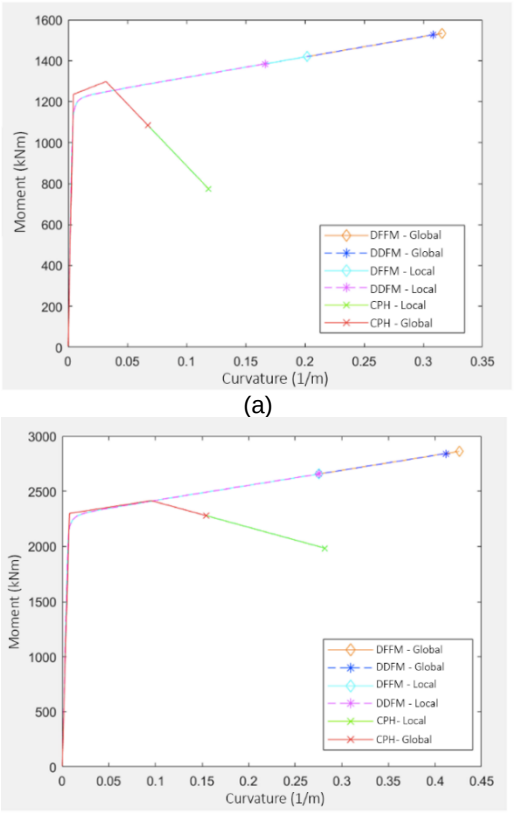

Figure 6 – Moment-curvature response: (a) at the left end of the first-floor beam; (b) the bottom end of the column at the first floor.

2.4.2 Non-linear Dynamic Analysis

The global and local response of the structure were submitted to the nonlinear dynamic analyses, evaluated respectively by displacement-time curves at the roof floor, shown in Figure 7, and moment-curvature curves, shown in Figure 9, however, none of the collapse criteria, local or global, was achieved.

Therefore, the global results seemed compatible in terms of maximum displacement, however, the CPH models (with and without degradation factors) present higher residual displacements, due to the resistance degradation parameters prevent the structure to

return to an undeformed position, however the differences are insignificant.

On the other hand, the local results, demonstrate that there is no compatibility between the models. The DFFM presents larger cyclic curvature curves than the other models. As well as, it was seen at the non-linear static analysis.

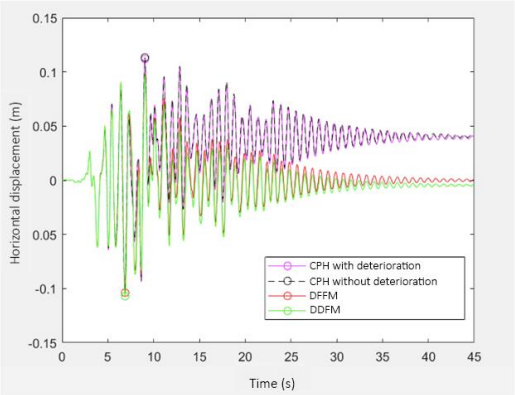

Figure 7 – Roof displacement curve along over the time.

3 Case Study: Steel structure PEF analysis using *OpenSees*

3.1 Fire Modelling Methods

Typically, a real fire goes through five distinct phases: ignition, growth, *Flashover,* burning and decay. It is also known the intermediate phase prior to the decay as *Post-Flashover,* as represented in Figure 8.

According to [9] two groups of fire modelling methods in compartments are contemplated: deterministic and probabilistic, described in Figure 10. The first, consists only of statistical forecasts on the growth phases of the fire. However, the second method is divided in three: computational fluid dynamics models, zone models, and manual calculation models. The last model refers to models defined in different phases of fire: *pre-flashover and post-flashover* fire models and travelling fire models.

NP EN 1991-1-2 [18] considers two groups of *post-flashover* models: nominal fire curves and natural fire models. The former are also mentioned in international standards such as ISO 834, [20], and ASTM E119, [15], while, the latter appears in the ASCE/SEI 7 standards, [14].

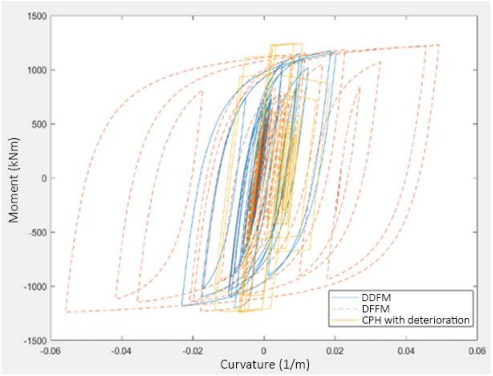

(a)

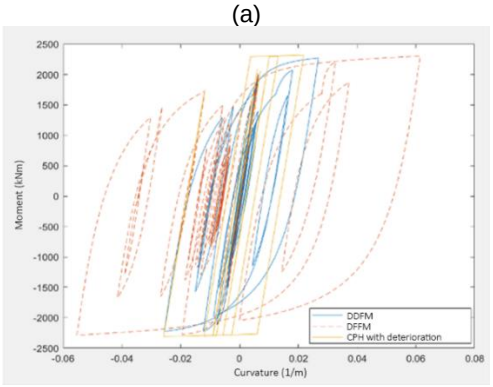

(b)

Figure 9 – Moment-curvature response: (a) at the left end of the first-floor beam; (b) the bottom end of the column at the first floor.

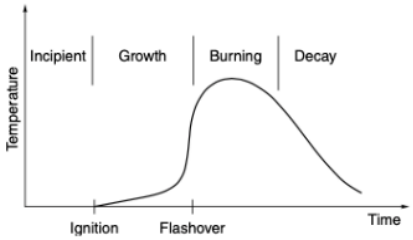

Figure 8 – Temperature-time curve (Fire phases).

Although the nominal curves do not represent any fire that may occur in real buildings, it was the model used in this simple study, in order to reduce the number of applicable parameters. Therefore, it was used the nominal fire curve model applied to steel elements defined according to the EN 1991-1-2 [18], also known as the ISO 834 curve. Also, to obtain the development of temperature in unprotected interior steel structures, assuming an equivalent distribution of uniform temperature in the cross-section, was given by EN 1993-1-2 [19].

Another essential aspect to be considered is the alteration of the characteristic properties of resistance and deformation of the material when subjected to temperature variation. So, the NP EN 1993-1-2 [19] provides 3 reduction factors for the stress-strain relationship for steel ate elevated temperatures: the reduction factor for the effective yield strength, $k_{y,\theta}$, the

reduction factor for the proportional limit, $k_{p,\theta}$, and the reduction factor for the slope of linear elastic range, $k_{E,\theta}$.

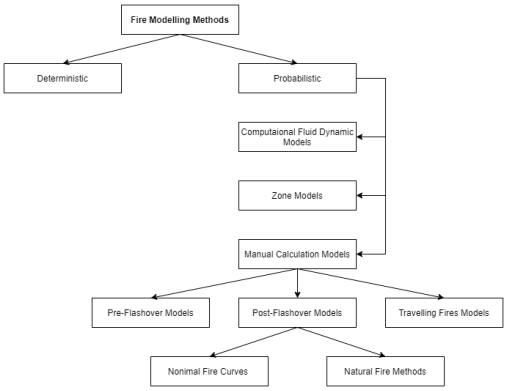

Figure 10 – Fire Modelling Methods.

3.2 Description of the structure

The case study consists in the evaluation of the resistance of a steel structure to the post-earthquake fire scenario, PEF. The aim of the study is to evaluate the progression of the damage of the structure, until the collapse, caused by the PEF scenario, by comparing with the resistance of the structure subjected only to fire conditions.

The structure under analysis corresponds to a frame, analyzed by Jelinek et al. [4] using the ABAQUS program. Jelinek et al. [4] also analyzed the structure in three scenarios: (i) earthquake; (ii) fire; and (iii) post-earthquake fire, so some results were compared, to validate de models using *OpenSees.*

The building represents the main frame of a residential steel building design by Zaharia et. al [13], according to the Romanian seismic code P100-1/2004 [21]. The load-bearing structure consists of an symmetric unprotected steel moment-resisting frame, with 5 elevated floors, and total building height of 18.5 m, as shown in Figure 11. The elements are made of S235 steel and all beam-column joints are assumed rigid. The frame is not insulated against fire, but is designed to withstand gravity and seismic load according to EN 1998-1 [16] (following the concept of strong column-weak beam). In particular, the design peak ground acceleration (PGA) is 0.32 g and the damping ratio of the structure is assumed equal to 1% (modelled here as Rayleigh damping). The design vertical loads are: the dead load of each floor (G_k =3.5 kN/m^2); the live load on regular floor (Q_k = 2.5 kN/m^2); and the live load on roof floor ($Q_{k,roof}$=1.5 kN/m^2). The load is calculated by using the accidental load combination for earthquake and fire. The Eurocodes indicate the combination factor of 0.3.

The nonlinear seismic response is analyzed through 6 earthquakes of different characteristics, scaling to the same peak acceleration. Later, in the PEF scenario, two of these earthquakes are selected to analyze the response. As for the fire scenario, standard curves (ISO 834) [20].

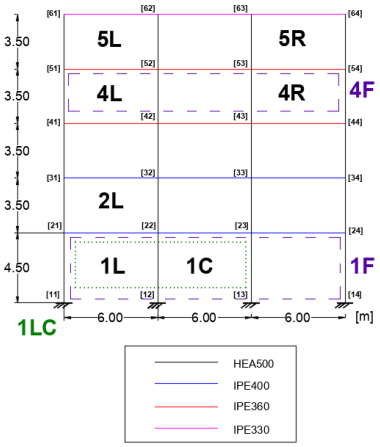

Figure 11 – Case study building geometry with dimensions in m and section profiles.

3.3 Finite Element and Material Models using *OpenSees*

3.3.1 Earthquake response analysis

The finite element and material models were the same presented in section 2.2.1. The beam and columns at the DFFM have 10 integration points. However, to reach the similar results with the DFFM, the DDFM beams and columns were discretized in 30 elements with 5 integration points each.

3.3.2 Fire and PEF response analysis

In the fire and PEF response analysis there were used the same beams and columns discretization. However, the material model used at the DFFM and DDFM models was a bilinear behaviour model without considering the Bauschinger effect. Ideally, it would be preferable to model the structure according *to the Giuffré-Menegotto-Pinto model,* but no successful analyses were achieved with this modeling. Also, the CPH model has not been executed because it is not possible to model Lignos and Krawinkler material model in *OpenSees*, under thermal action.

3.4 Collapse criteria

In addition to the plastic rotation capacity limit imposed to columns, according to the actualization of NP EN 1998-3, [6], presented in the Equation (1) and Equation (2), respectively, for the monotonic and cyclic analysis, used in this case to determine structure global time of collapse. It was applied the NP EN 1998-3 [17], former criteria for plastic rotation capacity that can be imposed to beams, illustrated in Table 2, to evaluate the local time of collapse.

Table 2 – Plastic rotation capacity, according to NP EN 1998-3, for damage limitation (DL), significant damage (SD), near collapse (NC) levels, [17].

Cross-section class	Limite state		
	DL	SD	NC
1	1.0 θ_y	6.0 θ_y	8.0 θ_y
2	0.25 θ_y	2.0 θ_y	3.0 θ_y

3.5 Results

3.5.1 Earthquake response analysis

The most important response outputs obtained at earthquake analysis were the comparison between maximum displacement and maximum residual strain, at each model, and the results of the ABAQUS study, for each seismic action. This analysis is presented in the Figure 12 and Figure 13, respectively. The ratios allow not only to compare the results between the model of the article, but also to compare the values between models. The CPH model presents the biggest difference in the results, in the Artificial earthquake, with 14% difference. Nevertheless, the difference is insignificant, and demonstrated compatible results between the modeling methods. However, the ratios of maximum residual strain do not demonstrate compatible results between the models, with a significant difference of 61% in the DDFM, at the Loma Prieta seismic action. This value would possibly improve the results obtained with the increase of discretization of the elements. It is possible to conclude that the results are compatible between models for the maximum displacement, however, to improve the results of extensions would require further discretization of the element.

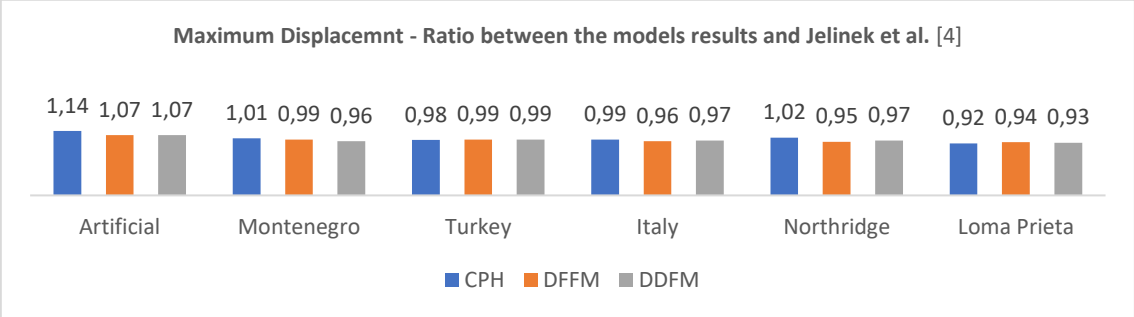

Figure 12 – Maximum displacement ratio between the models results and the Jelinek et al. [4] results.

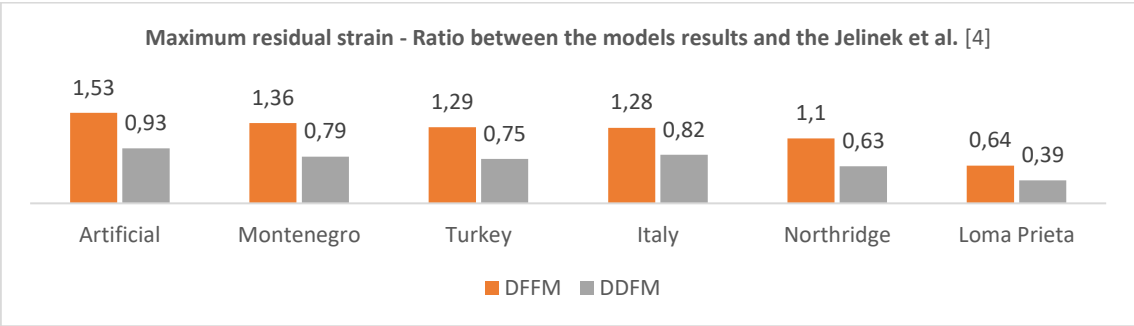

Figure 13 – Maximum residual strain- Ratio between the models results and the Jelinek et al. [4] results.

3.5.2 *Fire response analysis*

In fire analysis were analysed the 10 fire scenarios, illustrated in Figure 11, identified with a number indicating the floor number (1 to 5) and a letter indicating the position of the fire in the frame (R for right bay, C for center bay, L for left bay, and F for fire in the whole floor).

However, to one of the most critical scenarios, 1L, that has an asymmetric loading, it was determined the global and local time of collapse according to the plastic rotation capacity limit, respectively, imposed to the columns and beams. The result of the global collapse time is 23.77 min, and the local collapse time is 13.90 min.

The column limit is based on the actualization of NP EN 1998-3, [6], and the beam limit is according to the NP EN 1998-3 [17], for the NC limitation, for the section profile class 1. Despite the small difference between the global and local time of collapse, the most conditional is the global collapse. In comparison to the global collapse time presented by Jelinek et al. [4] was 28.0 min, it is possible to verify that the time obtained for the global collapse, according to the NP EN 1998-3 [17] criterion, is lower, however, the difference is not significant.

3.5.3 *PEF response analysis*

To the evaluate the resistance in PEF response analysis where executed the model analysis to the scenarios 1L-A e 1L-M, for the DFFM. Due to the low residual deformations of the seismic action, it was not evident the reduction of the structure resistance to fire, in relation with the seismic damage. Therefore, it was analysed the reduction of the structures, with the increase of seismic intensity scale factor, as shown in Figure 14 and Figure 17, respectively, the global and local time of collapse.

The criteria to determine the global and local time of collapse are the same described in section 3.4. To analyse the order of magnitude of the residual seismic deformations that causes the reduction of the time of collapse, were illustrated the maximum residual seismic roof drift, and at first floor, respectively, in Figure 15 and Figure 16.

It is very interesting to observe the relationship between the decreasing of the global collapse time, obtained by the plastic rotation capacity limitations [17] for columns, and the increasing maximum seismic residual deformations. Between 2% and 3% of residual *drift* of seismic action, the structure already presents global collapse at the end of the earthquake, that is, the action of fire no longer influences the collapse of the structure.

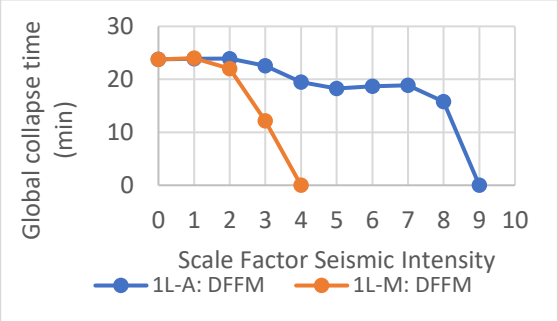

Figure 14 – Global collapse time for different seismic intensities, for 1L-A and 1L-M scenarios, with DFFM.

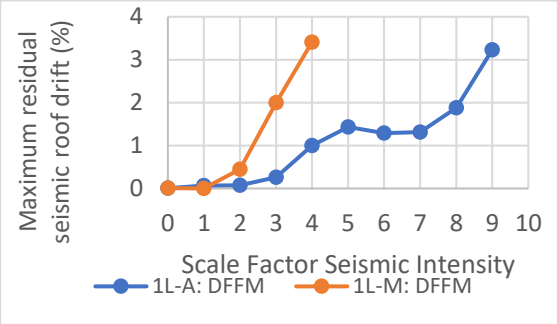

Figure 15 – Maximum residual seismic roof drift for different seismic intensities, for 1L-A and 1L-M scenarios, with DFFM.

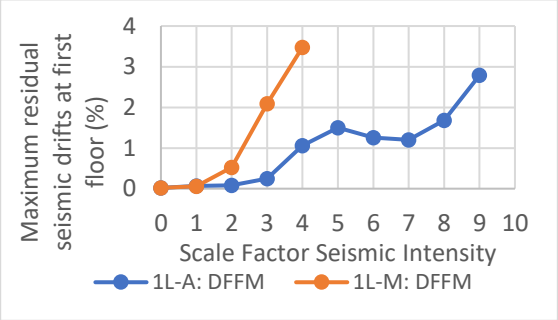

Figure 16 – Maximum residual seismic drift at first floor for different seismic intensities, for 1L-A and 1L-M scenarios, with DFFM.

On the other hand, the collapse time determined at the beam of the compartment 1L, as shown in Figure 17, is slightly affected with the increase of seismic damage. Demonstrating that it is not influenced by the seismic action before.

So, in Figure 18, is illustrated the vertical residual seismic displacement, in comparison with the vertical displacement at the local collapse, for an increasing seismic intensity, at the beam's midsection. And it can be observed,

a relation with the local time of collapse. The increase of the vertical residual seismic displacement, at this section, is not significant (demonstrating that the vertical deformation of beam is not affected by the seismic damage), justifying the local collapse time curve small differences.

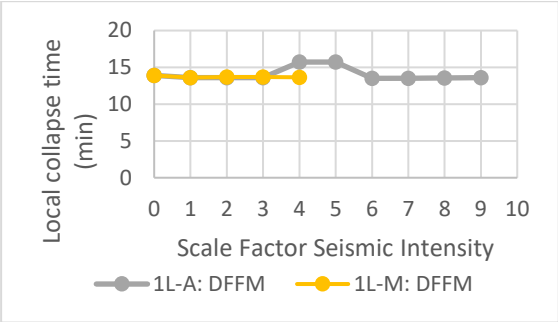

Figure 17 – Local collapse time for different seismic intensities, for 1L-A and 1L-M scenarios, with DFFM.

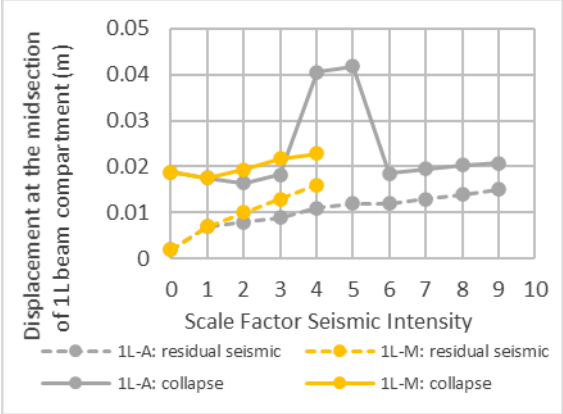

Figure 18 – Residual seismic displacement and collapse displacement, at midsection of 1L beam compartment, for different seismic intensities, for 1L-A and 1L-M scenarios, with DFFM.

In general, the most critical collapse time is the local collapse time for both scenarios, however, for higher scale factor seismic intensities the columns collapse is conditioning, demonstrating the influence of the seismic intensity on the structure fire resistance.

It can be observed that the Artificial earthquake and the Montenegro earthquake present different responses. The Montenegro earthquake, with lower scale factor intensity reaches higher deformations, unlike the Artificial earthquake. The Montenegro earthquake, with a scale factor equal to 1, causes more damage to the structure than the Artificial earthquake. It is possible to observe by the accelerograms of these earthquakes, that the Artificial earthquake has maximum acceleration values below the peak acceleration values of the Montenegro earthquake. This reason proves to cause greater damage to the structure, with the Montenegro earthquake, as it also demonstrated by the higher residual drifts, compared to the different earthquakes.

4 Conclusions

Nonlinear dynamic analysis delivers a residual state of the more realistic structure by following a history of real or artificial accelerations. As opposed to nonlinear static analysis, where lateral loads are applied, in the same direction, throughout the analysis. It was demonstrated the differences between concentrated and distributed plasticity models in a structure subject to seismic action. It is important to note that the different modeling approaches imply different results, which may not be appropriate in some analyses.

At seismic and fire analysis, local and global level differences were observed between models resulting from material behavior models, more specifically, how material resistance degradations are considered. Those differences must minimize considering higher discretization. The highest disadvantage of the distributed plasticity model with displacement formulation is that it needs much higher computational effort to obtain results similar to formulation in force model, that consequently increases the analysis time. The biggest disadvantage of *OpenSees* is that it is difficult to achieve the global collapse of the structure due to problems of numerical convergence.

In an asymmetric scenario of fire loading, at the first floor of the structure, one of the most critical scenarios for structures submitted to fire actions, it was showed that the criterion of plastic rotation capacity according to the update of NP EN 1998-3 [6], in the columns, produces very interesting and suitable results on evaluating the global time of collapse, due to the almost inverted response of the deformations increase and the decrease of collapse time, for different seismic intensities.

Also, the local collapse time results, according to NP EN 1998-3 [17], showed a correlation with the vertical residual seismic displacement at the beam midsection. Even so, it was demonstrated that the beam's vertical displacement is not affected by the seismic damage increase.

In this study, the local collapse proved to be conditioning in both the fire situation and the PEF events, however for higher seismic damage the column deformations were critical to the structures collapse.

Bibliography

- Articles

[1] Baker, Gregory B., Collier, Peter C.R., Abu, Anthony K., Houston, Brent J., *Post-earthquake structural design for fire-a New Zealand perspective*, 7th International Conference on Structures in Fire, M. Fontana, A. Frangi, M. Knobloch (Eds.), Zurich, Switzerland, June 6-8, 2012.

[2] Behnam, B., & Ronagh, H. R., *Post-Earthquake Fire performance-based behavior of unprotected moment resisting 2D steel frames*. KSCE Journal of Civil Engineering, 19(1), 274-284, 2015.

[3] Della Corte, G., Landolfo, R., & Mazzolani, F. M., *Post-earthquake fire resistance of moment resisting steel frames*, Fire Safety Journal, 38(7), 593-612, 2003.

[4] Jelinek, T., Zania, V., & Giuliani, L., *Post-earthquake fire resistance of steel buildings*, Journal of Constructional Steel Research, 138, 774-782, 2017.

[5] Jiang, L., Dai, X., Usmani, A., & Kamath, P., *OpenSees-based integrated tool for modelling structures in fire*, In The First International Conference on Structural Safety under Fire & Blast, 461-468, 2015.

[6] Lignos, D. G., & Hartloper, A. R., *Steel column stability and implications in the seismic assessment of steel structures according to Eurocode 8 Part 3*, Stahlbau, 89(1), 16-27, 2020.

[7] Lignos, D., Krawinkler, H., *Deterioration Modeling of Steel Components in Support of Collapse Prediction of Steel Moment Frames under Earthquake Loading*, Journal of Structural Engineering, 137(11): 1291-1302, 2011.

[8] McKenna, F. T., *Object-oriented finite element programming: Frameworks for analysis, algorithms and parallel computing*, A dissertation submitted in partial satisfaction of the requirements for the degree of Doctor of Philosophy in Engineering – Civil Engineering in the Graduate Division of the University of California, Berkeley,1999.

[9] Rosário, Rúben Miguel Paulos Ribeiro, *Modelação Não Linear de Estruturas Metálicas e Mistas em Situações de Incêndio no Software OpenSees*, Dissertação para obtenção do Grau de Mestre em Engenharia Civil, Faculdade de Ciências e Tecnologia, Universidade Nova de Lisboa, 2014.

[10] Terrenzi, M., Spacone, E. and Camata, G., *Comparison Between Phenomenological and Fiber-Section Non-linear Models*, Frontiers in Built Environment, 6, 38, 2020.

[11] Vila Real, P. M. M., Lopes, N., Silva, L. S., Piloto, P., and Franssen, F. M., *Numerical modelling of steel beam-column in case of fire-comparisons with Eurocode 3.,* Fire Saf. J., 39(1), 23–39, 2004.

[12] Wellington Lifelines Group, *Fire following earthquake; identifying key issues for New Zealand,* Wellington Lifelines Group, Wellington, New Zealand, 2002.

[13] Zaharia, R., & Pintea, D., *Fire after earthquake analysis of steel moment resisting frames*, International Journal of Steel Structures, 9(4), 275-284, 2009.

- Standards

[14] ASCE, SEI 7-10 Minimum Design Loads for Buildings and Other Structures, American Society of Civil Engineers, Reston, VA, 2013.

[15] *ASTM Designation E 119-88, Standard Methods of Fire Tests of Building Construction and Materials*, Section 4, Vol. 04.07, American Society for Testing and Materials, Philadelphia, PA, 1994.

[16] CEN. EN 1998-1: 2004, *Eurocode 8: Design of structures for earthquake resistance - Part 1: General rules,*

seismic actions and rules for buildings, Comité Européen de Normalisation, 2004.

[17] CEN. EN 1998-3: 2005, *Eurocode 8: Design of structures for earthquake resistance – Part 3: Assessment and retrofitting of buildings*, Comité Européen de Normalisation, 2005.

[18] IPQ. NP EN 1991-1-2:2010*, Eurocódigo 1 – Acções em estruturas Parte 1-2: Acções gerais. Acções em estruturas expostas ao fogo,* 2010.

[19] IPQ. NP EN 1993-1-2: 2010, *Eurocódigo 3 – Projecto de estruturas de aço. Parte 1-2: Regras gerais. Verificação da resistência ao fogo*, Instituto Português da Qualidade, 2010.

[20] *ISO 834 Fire-resistance tests — Elements of building construction*, 1999.

[21] P100-1/2004, *Seismic design code-Part 1: Rules for buildings Indicativ P100-1/2004*, Buletinul Constructiilor, Vol. 5 (in Romanian), 2005.